Modelling and Simulation of Radial Spruce Compression to Optimize Energy Efficiency in Mechanical Pulping

Carolina Moilanen[1], **Tomas Björkqvist**[2], **Markus Ovaska**[3], **Juha Koivisto**[3], **Amandine Miksic**[3], **Birgitta Engberg**[4], **Lauri Salminen**[5], **Pentti Saarenrinne**[1], **Mikko Alava**[3]

1) Tampere University of Technology, Department of Mechanical Engineering and Industrial Systems, P.O. Box 589, FI-33101 Tampere, Finland
2) Tampere University of Technology, Department of Automation Science and Engineering, P.O. Box 692, FI-33101 Tampere, Finland
3) Aalto University, School of Science, Department of Applied Physics, P.O. Box 11100, FI-00076 Aalto, Finland
4) Mid Sweden University, Department of Chemical Engineering, Holmgatan 10, SE-85170 Sundsvall, Sweden
5) VTT, current at A Fredrikson Research and Consulting Ltd, Vähäkuja 2 A 2, 40520 Jyväskylä, Finland

ABSTRACT

Energy efficiency of mechanical pulping is rather low. One possibility to facilitate design of more energy efficient defibration is to model and simulate wood compression. This paper presents an effort to model the behavior of Norwegian spruce in radial compression at defibration circumstances. To identify strain rate dependent properties, compression tests were conducted at both quasi-static conditions and at high strain rate. All tests were done at relevant moisture content and up to defibration zone temperatures and strain rates. Additionally the tests were performed both on native wood and on pre-fatigued wood to include behavior dependency of fatigue. The compression tests were monitored on fiber level to separately model behavior of early- and latewood. The chosen continuum model structure for earlywood and latewood was Voight-Kelvin to enable explicit viscous behavior conditioned by strain rate in parallel to the elastic behavior. The presented model is the first wood compression behavior model individually for earlywood and latewood that is based on wood experiments at industrial defibration circumstances. The influences of temperature and pre-fatigue rise are both softening as expected. The utilization of the compression model was demonstrated in an initial multilayered wood compression simulation.

INTRODUCTION

The energy consumption of mechanical pulping is a burden. High electrical energy consumption is not only a disadvantage for the total production economy, but also harmful for the reputation of an otherwise environmentally friendly industry based on renewable resources. The low observability of fundamental actions in the defibration zone of mechanical pulping processes has prevented a straightforward design development to achieve high energy efficiency in defibration. A lot of attempts to clarify the fundamental phenomenon in the defibration zone, both on fiber and conditions level, has been made during decades. To mention some, pioneer empirical work started with local temperature measurement inside wood blocks during grinding [1] and has progressed through high speed video inside refiner gap [2,3] and culminates at the moment in on-line refiner bar temperature and force measurements [4,5]. All empirical work has increased the understanding of basic phenomena in mechanical pulping and supported significant progress in process development. In parallel to the on-site empiric process exposure, intensive research has been done to understand the mechanical behavior of wood at defibration circumstances. This work is mainly about laboratory wood measurements, starting with pioneer work at modest conditions [6,7,8] but later shifting, along with developing measurement techniques, to real defibration circumstances where wood moisture, temperature and wood deformation rates are similar to those in defibration [9,10,11,12,13]. Comprehensive knowledge of relevant wood behavior enables modelling of wood actions and further simulation of wood processing [14,15,16,17,18]. This research has improved the understanding of mechanical pulping and also supported the already seen significant development of processes. The ultimate goal is to be able to simulate complete defibration action processes and thereby to enable rational process optimization virtually. The wood behavior research has revealed that wood strain is the main mechanical action producing fatigue for the needed fiber flexibility required in end products [19,20,21,22,23,24]. As wood has viscoelastic features mechanical energy used for strain achievements will always partly dissipate into heat energy. The challenge then becomes to design a mechanical process for needed fatigue development but with as little energy dissipated into heat as possible.

This paper presents an international joint effort to model the behavior of Norwegian spruce in radial compression at defibration circumstances. To identify strain rate dependent properties, compression tests were conducted at both quasi-static conditions and at high strain rate. All tests were done at relevant moisture content and up to defibration zone temperatures and strain rates. Additionally the tests were performed both on native wood and on pre-fatigued wood to include behavior dependency of fatigue. The compression tests were monitored on fiber level to separately model behavior of early- and latewood. The chosen continuum model structure for earlywood and latewood was Voight-Kelvin to enable explicit viscous behavior conditioned by strain rate as time dependency in parallel to the elastic behavior. To achieve these the research teams worked tight together and utilized amongst other things the following expertise; pre-fatigue treatment at VTT, quasi-static compression tests at Aalto University, high strain rate compression tests at Mid Sweden University and high-speed imaging and image processing at Tampere University of Technology. This paper is based on two journal articles [12,13] and additionally includes initial simulation utilization of the developed wood compression model.

MATERIAL AND METHODS

Wood Material

The measurements were conducted on fresh Norway spruce samples from large trees from Myskylä, in southern Finland, see Fig. 1. All samples were from 4-8 m height and from defect-free sapwood that was cut fresh and stored frozen. The samples were removed from the freezer at least 24 h before use and left to thaw in a sealed container in room temperature. Samples with low latewood curvature were chosen. The quasi static compression tests were conducted on samples that were approximately 5 mm x 5 mm x 5 mm, while high strain rate testing was conducted on sample that were approximately 6 mm in the radial direction, 12 mm in the tangential direction and 12 mm in the longitudinal direction. The raw material used in mechanical pulping is preferable wet (moisture content around 50 %). The moisture content of the samples was approximately 30 % which corresponds to the fiber wall saturation level. Higher moisture content would result in free water in the fiber lumens, which would cause problems with the image based method. The moisture content was approximated before the measurement by comparing the density of the sample to that of a dry sample from the same larger piece of wood. Part of the samples was pre-fatigued by 20 000 strain pulses at 500 Hz in a device described in [25,26]. This pre-fatigue treatment can be considered to be intensive. The pre-fatigued treatment was applied from the outside of the log.

The samples were adjusted with a microtome before the testing procedure in order to get a flat and smooth surface and ensure that the opposite surfaces in the loading direction were parallel. Slanted sample surfaces may result in perpendicular forces, surface friction and eventually sample slip or movement. Four samples were tested at each temperature and strain rate for both native and fatigued wood. One pre-fatigued sample at 100 °C and at high strain rate could not be successfully analyzed and therefore, results from only three samples are presented. [12,13]

Fig. 1 Wood raw material.

Wood Testing

The material model developed here takes the strain rate into account and required material testing at two different strain rates, quasi static compression with a strain rate of approximately 0.004 s^{-1} and high strain rate compression with global stain rates of 800 - 2400 s^{-1} (lower strain rate at high temperature). [12,13]

Quasi-static compression tests. The quasi static testing was conducted in an Instron E1000 tensile testing machine. At room temperature, the wood samples were tested in air and submerged in water. To prevent drying the wood samples were only tested submerged in water at 80 °C. The quasi static tests at 80 °C are compared to the high strain rate tests at 100 °C and will be referred to as high temperature tests.

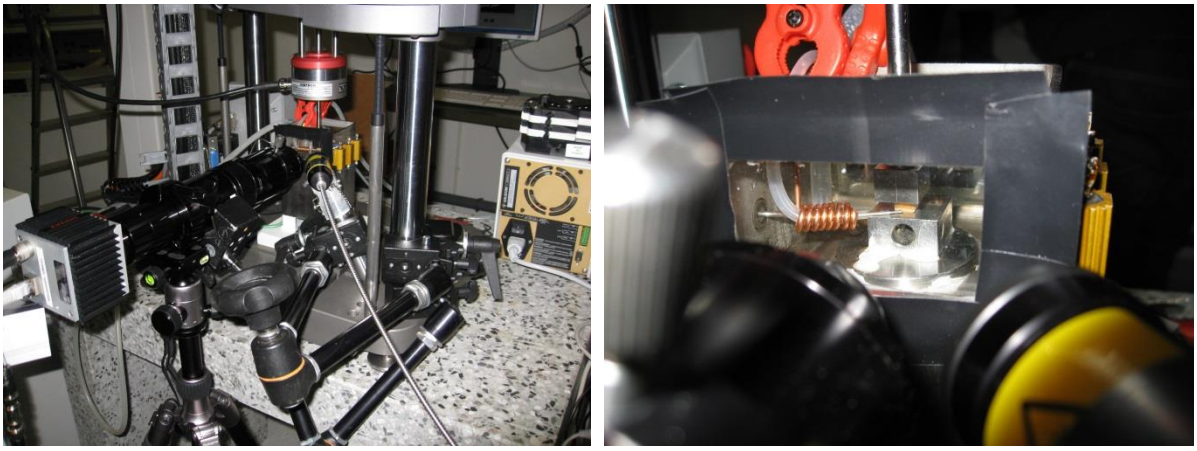

Fig. 2. Quasi-static compression testing setup.

High strain rate compression tests. The split-Hopkinson pressure bar is commonly used for high strain rate material testing. The high strain rate testing was here conducted in a split-Hopkinson pressure bar that was encapsulated in a thermally insulated pressure vessel. The split-Hopkinson device was heated by saturated steam to 100 °C. Details of the split-Hopkinson testing technique are presented in [27,28,29] and the encapsulated split-Hokinson device is presented in [10].

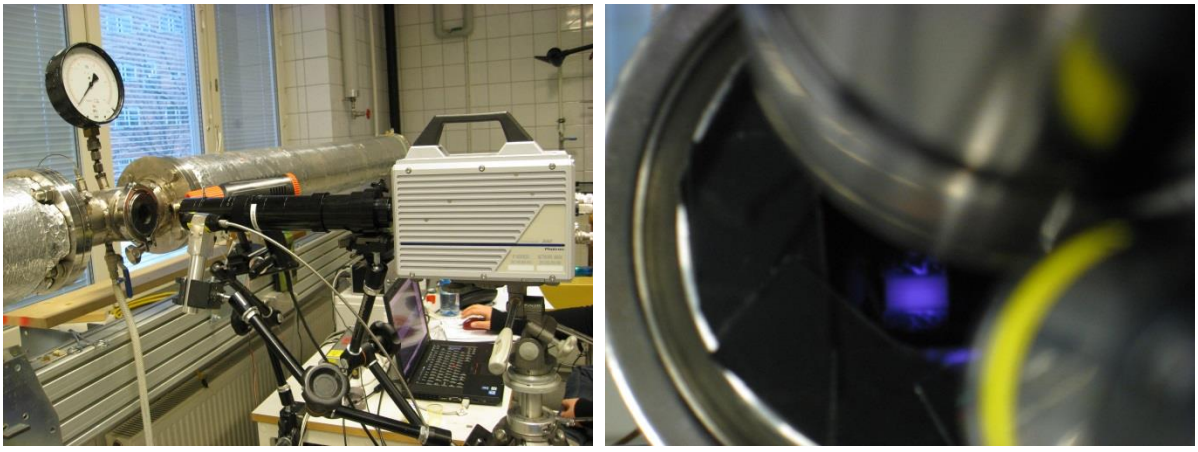

Fig. 3. High strain rate compression testing setup.

Image acquisition. An Infinity K2 long distance microscope was used with an Imperx Lynx GigE camera for the quasi static material tests and with a Photron SA5 high speed camera for the high strain rate tests. A framerate of 2 Hz was used during the quasi static tests while the high strain rate tests required a framerate of 50 000 – 100 000 Hz. The resolution was 2.9 - 4.0 µm/pixel for the high speed images and 2.1 µm/pixel in the quasi static images.

Local strain analysis. An image based method presented in [11] was used to analyze earlywood and latewood compression. The analyzed area was 32x32 pixels for the quasi static images and 16x16 for the high strain rate images. The image correlation was less accurate for the water submerged samples due to reduced contrast in the images. The free water in the lumen decrease the opacity of the surface and the light is reflected diffusively from varying depth of the surface.

Global stress determination. The stress was calculated from the strain registered by strain gauges in the high strain rate tests while the stress was measured with a load cell in the quasi static tests.

Dynamic Wood Compression Model

The compression rate affects the response of wood significantly. The expected difference between quasi static compression and high strain rate compression is illustrated in Fig. 4. In this example, the two tests have the same yield limit and densification limit but the elastic modulus and the densification modulus differ. The biggest difference for fiber saturated samples is in the elastic part of the stress-strain curve [9].

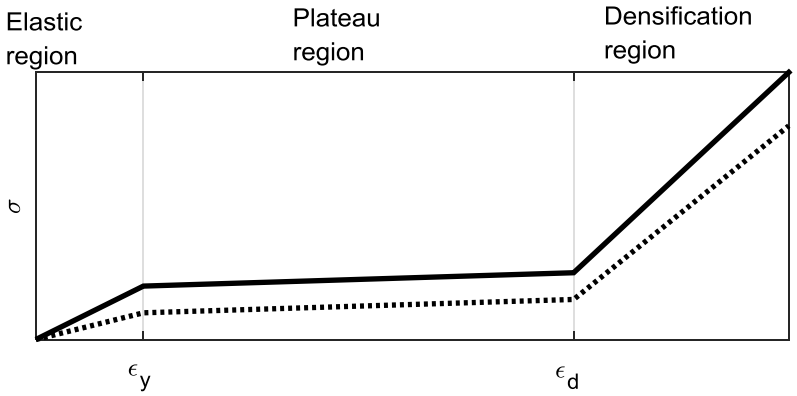

Fig. 4 Simplified stress-strain curve for quasi static compression (dotted line) and high strain rate compression (solid line), where ε_y denotes the yield limit and ε_d denotes densification limit

A simple three part linear model was presented in [12] to describe earlywood compression. This model did not take the strain rate explicitly into account i.e. the model was only accurate for the strain rate in the experiments. We assume here that wood behaves like a Voigt-Kelvin solid. For Voigt-Kelvin solids, the stress is a sum of two parts: one proportional to the strain and one proportional to the strain rate [30]. The part proportional to the strain rate represents internal friction, i.e. viscous effects. The three part material model was modified by adding the term $\eta\dot{\varepsilon}$ that is assumed to be linearly proportional to the strain rate, as presented in Eq. 1,

$$\sigma_{EW} = \begin{cases} E_e^{EW}\varepsilon_{EW} + \eta^{EW}\dot{\varepsilon}_{EW} & \varepsilon_{EW} \le \varepsilon_y^{EW} \\ E_e^{EW}\varepsilon_y^{EW} + \eta^{EW}\dot{\varepsilon}_{EW} + E_p^{EW}\left(\varepsilon_{EW} - \varepsilon_y^{EW}\right) & \varepsilon_y^{EW} < \varepsilon_{EW} \le \varepsilon_d^{EW} \\ E_e^{EW}\varepsilon_y^{EW} + \eta^{EW}\dot{\varepsilon}_{EW} + E_p^{EW}\left(\varepsilon_d^{EW} - \varepsilon_y^{EW}\right) + E_d^{EW}\left(\varepsilon_{EW} - \varepsilon_d^{EW}\right) & \varepsilon_{EW} > \varepsilon_d^{EW} \end{cases}, \quad (1)$$

where σ_{EW} is the stress in earlywood, E_e^{EW} is the elastic modulus in earlywood, E_p^{EW} is the plateau modulus in earlywood, E_d^{EW} is the densification modulus in earlywood, ε_y^{EW} is the earlywood yield limit, ε_d^{EW} is the earlywood densification limit and η^{EW} the viscous parameter for earlywood. The variables in the model are the strain rate in earlywood $\dot{\varepsilon}_{EW}$ and the strain in earlywood ε_{EW}. The internal friction could be slightly different in the elastic, plateau and densification regions since the mechanism of the compression changes, however here the viscous effect was modelled as one single step to keep the model simple.

The latewood compression can be assumed to be linear elastic, as it was also in [12]. In order to take the strain rate into account, a similar term $\eta\dot{\varepsilon}$ was added as in Eq. 1,

$$\sigma_{LW} = E_e^{LW}\varepsilon_{LW} + \eta^{LW}\dot{\varepsilon}_{LW} \quad (2)$$

where σ_{LW} is the stress in latewood, E_e^{LW} is the elastic modulus in latewood, η^{LW} is the viscous parameter for latewood, $\dot{\varepsilon}_{LW}$ the strain rate in latewood and ε_{LW} is the strain in latewood.

The parameters E_e^{EW}, E_p^{EW}, E_d^{EW}, ε_y^{EW}, ε_d^{EW} and E_e^{LW} were fitted by optimization from the quasi static tests first, where the strain rate was practically zero (the high strain rate compression was 800-2400 s^{-1} while the quasi static compression strain rate was 0.004 s^{-1}). The models fitted based on the quasi static experimental data is referred to as quasi static models. The parameters η^{EW} and η^{LW} were then used to fit the models to the high strain rate experimental data. The strain rate used was the local strain rate, i.e. time variant strain rate in earlywood or latewood. The models including the viscous parameter effect is referred to as dynamic models. The material parameters are dependent on both temperature and fatigue state. The parameter optimization was made for all parallel samples simultaneously with the least square method in MATLAB (lsqcurvefit) [13].

RESULTS AND DISCUSSION

The results section is divided into two main parts. The native wood compression models for earlywood and latewood at two temperatures, both the static and the extended dynamic version, is derived first and then the earlywood and latewood models for fatigued wood, also at two temperatures and as a static and extended dynamic version, is derived. [13]

Initially we will analyze the effect of submerging the wood sample into a heated water bath during the quasi static compression tests at elevated temperatures to prevent drying. During the room temperature tests samples were both tested submerged in the water bath and in air to investigate the effect of the water bath. The global stress strain curves for native samples tested in air and in water are compared in Fig. 5a and the earlywood stress strain curves in Fig. 5b.

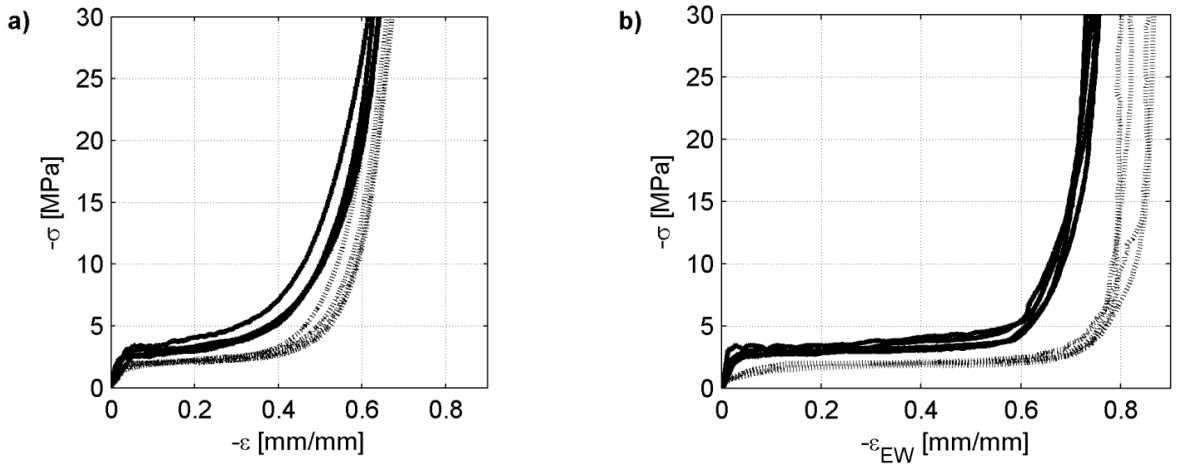

Fig. 5 a) Global stress strain curves and b) earlywood stress strain curves for native samples tested in air (solid line) and submerged in water (dotted line) at room temperature.

At room temperature, the samples submerged in water were slightly softer than the samples that were tested in air. The difference is more distinct in the earlywood stress strain curves (Fig. 5b) than in the global stress strain curves (Fig. 5a). The difference is assumed to be less significant at higher temperatures, when temperature starts to dominate

the softening. Furthermore, the quasi static testing (using samples submerged in water) was conducted at 80 °C for safety reasons while the high strain rate testing devise was heated with steam to 100 °C. The softening of wood between 80 °C and 100 °C is according to [21] low, the following more significant softening occurs above 150 °C and is due to thermal degradation. Thus, we know that the water softening will reduce the effect of the lower temperature in the quasi static testing compared to the high strain rate testing but we do not know how close we get to the actual quasi static compression behavior of wood with 30 % moisture content at 100 °C.

Compression Model with Static and Dynamic Terms for Native Wood

The densification region was not reached in the high strain rate tests, therefore the material model was reduced to a two part linear model with the material parameters E_e^{EW} , E_p^{EW} , ε_y^{EW} , E_e^{LW} , η^{EW} and η^{LW}. The densification region was reached during the quasi static tests, but the stress strain curves were cut off after the plateau region in the analysis and in the figures since the densification region was not included in the dynamic model.

Earlywood model. The earlywood model for earlywood part of native wood is compared to earlywood test results in Figs. 6-8. The quasi static model is presented in Fig. 6 and the high strain rate model in Figs. 7 and 8. The quasi static model is included in Figs. 7 and 8 to highlight the effect of the dynamic parameter.

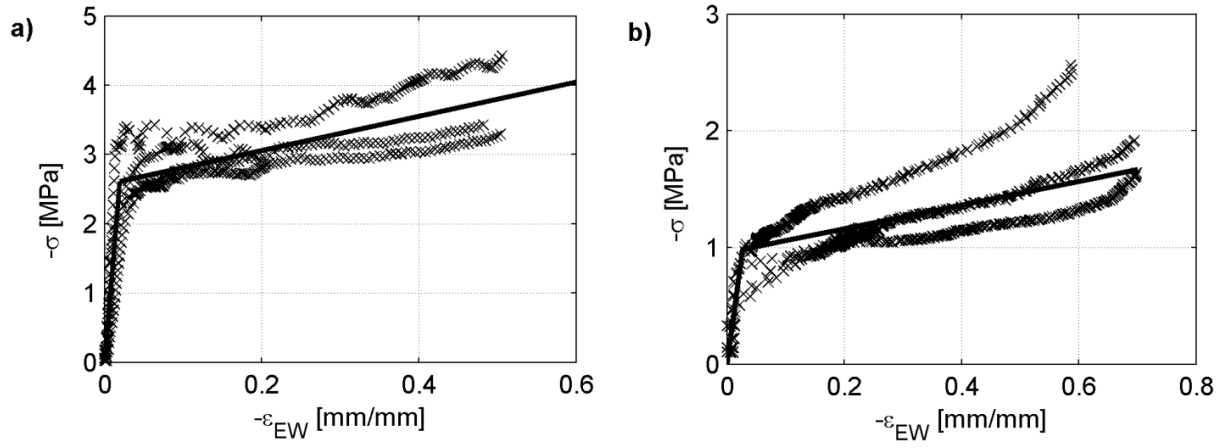

Fig. 6 Stress strain curves based on the quasi static earlywood model (solid line) and experimental data (x) from compression tests at a) room temperature and b) high temperature.

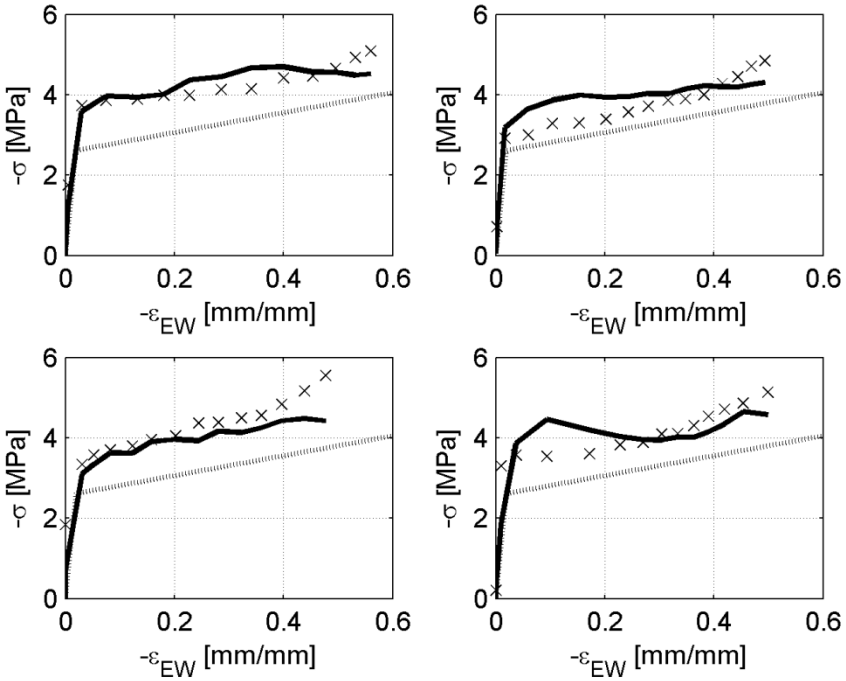

Fig. 7 Stress strain curves for earlywood based on the dynamic model (solid line), the quasi static model (dotted line) and experimental data (x) for four native samples tested at high strain rate at room temperature.

The reason why the dynamic model fluctuates is the variations in the local strain rate during the high strain rate experiments. The individual local strain rates were used simultaneously for all parallel samples when fitting the model and when testing the models visually only the corresponding individual strain rates was used. Similar fluctuating stress can be seen in all high strain rate tests in this study.

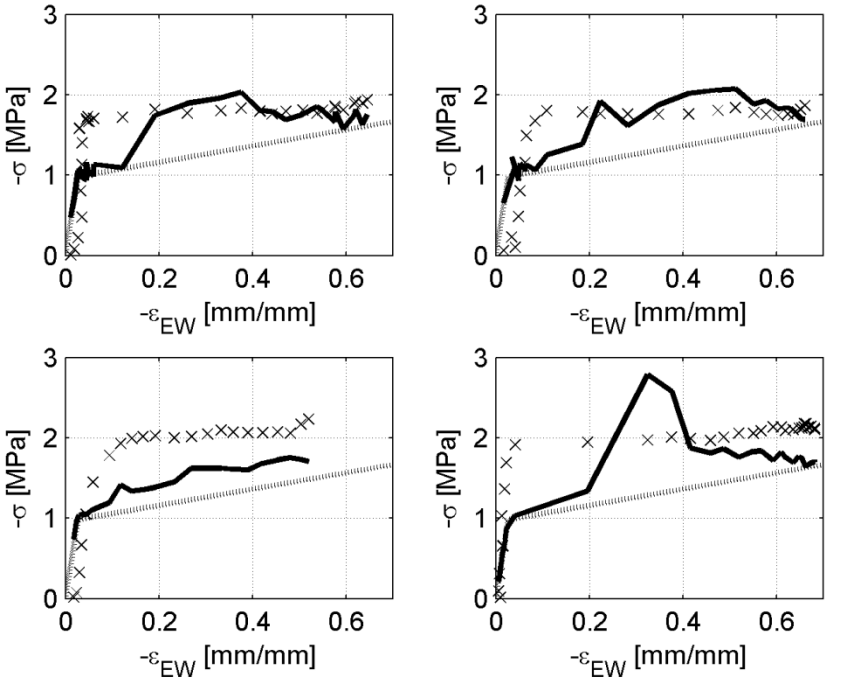

Fig. 8 Stress strain curves for earlywood based on the dynamic model (solid line), the quasi static model (dotted line) and experimental data (x) for four native samples tested at high strain rate at high temperature.

The individual stress strain behavior at high strain rate compression can especially be seen in the high temperature experiments. The model accuracy would have been favored with more successful experiments but already these have demanded huge amount of experimental work. The experimental results are in line with the expectations of strain rate influence shown in Fig. 4 and the softening of wood at higher temperature is clearly seen.

Latewood model. The quasi static model for latewood is presented together with experimental data in Fig. 9 and the dynamic model for latewood in Figs. 10 and 11. The quasi static results are included in Figs. 10 and 11 to highlight the difference between the models.

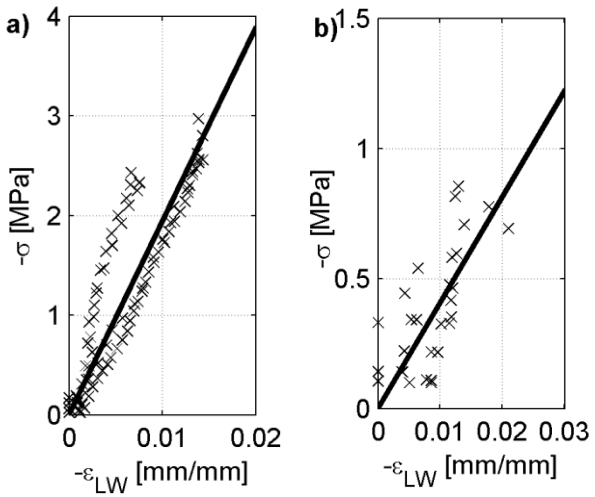

Fig. 9 Stress strain curves based on the quasi static latewood model (solid line) and experimental data (x) from compression tests at a) room temperature and b) high temperature.

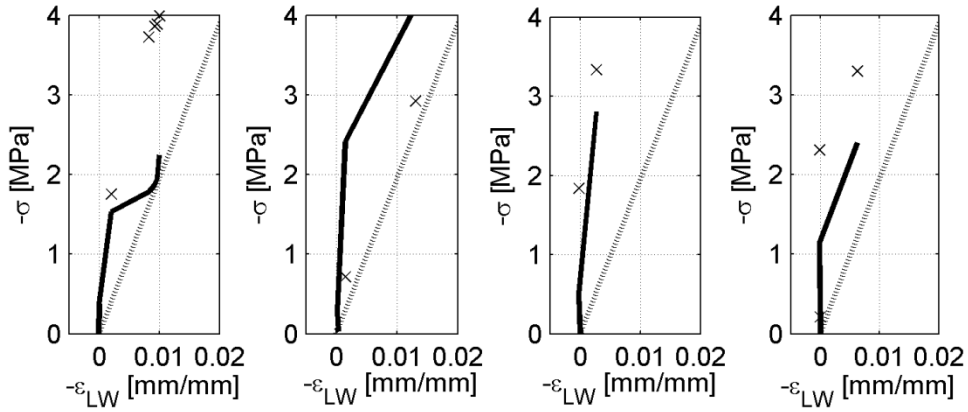

Fig. 10 Stress strain curves for latewood based on the dynamic model (solid line), the quasi static model (dotted line) and experimental data (x) from high strain rate testing of four native samples at room temperature.

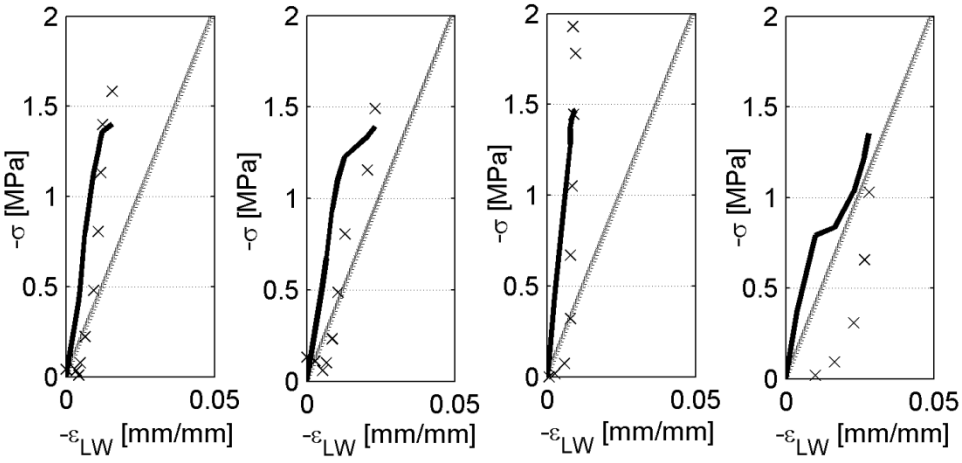

Fig. 11 Stress strain curves for latewood based on the dynamic model (solid line), the quasi static model (dotted line) and experimental data (x) from high strain rate testing of four native samples at high temperature

Also the latewood results shows strong softening due to high temperature and higher stress values as an effect of the high strain rate.

Compression Model with Static and Dynamic Terms for Fatigued Wood

Initially in this section we will analyze fatigue development. The effect of low strain rate fatigue was investigated by advancing cyclic compressions with increasing maximum strain that was synchronized with images. The global stress strain curve from the cyclic compressions of a native wood sample is presented in Fig. 12a and the corresponding curve for image based earlywood strain is presented in Fig. 12b. The numbers I-III in Fig. 12 marks the positions during loading where the images in Fig. 13 were captured. The stress strain curves from quasi static single compression tests of native samples at room temperature are plotted with dotted lines in Fig. 12 to emphasize that the upper part of the cyclic curve corresponds to that of native wood subjected to one single compression.

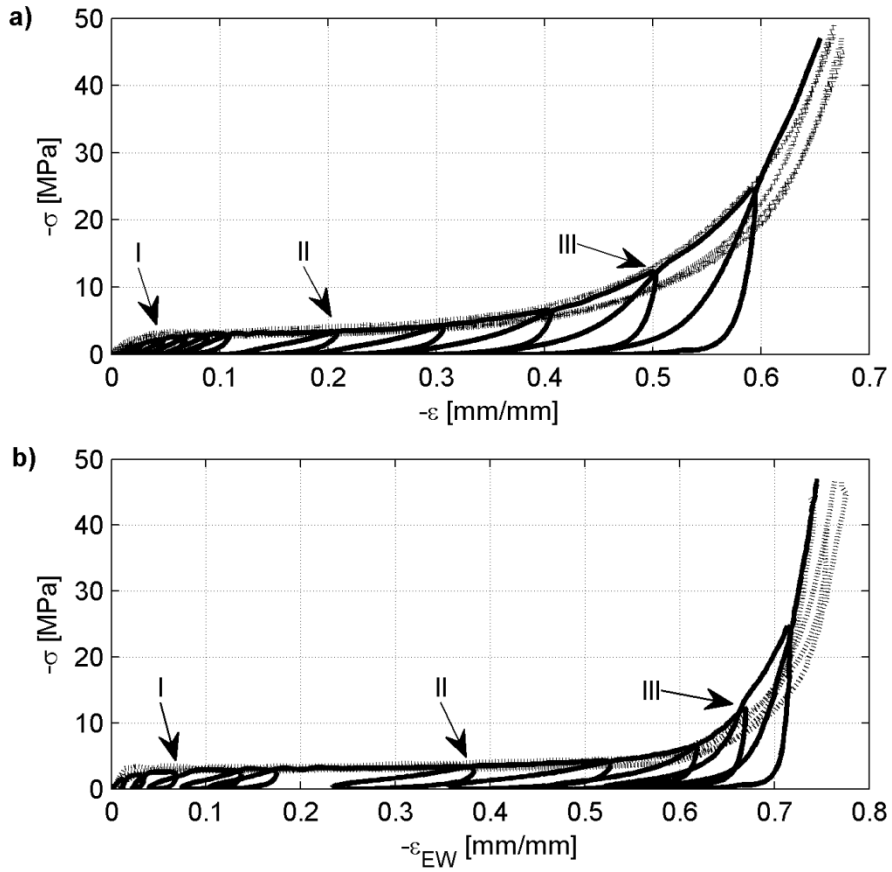

Fig. 12 Stress strain curves from quasi static cyclic loading of native wood (solid line) and single loading of native wood (dotted line) at room temperature a) global strain b) image based earlywood strain, where the numbers I-III indicates the positions where the images in Fig. 13 were captured.

Figs. 13a, b and c show two images captured at the same strain level during two consecutive compression cycles. The image to the left in Fig. 13a is captured at maximum strain in the end of the second compression cycle and the image to the right in the middle of the third compression cycle at the same strain level. The images in Fig. 13b are correspondingly captured in the end of the sixth compression cycle and in the middle of the seventh compression cycle and the images in Fig. 13c are captured in the end of the ninth compression cycle and in the middle of the tenth compression cycle.

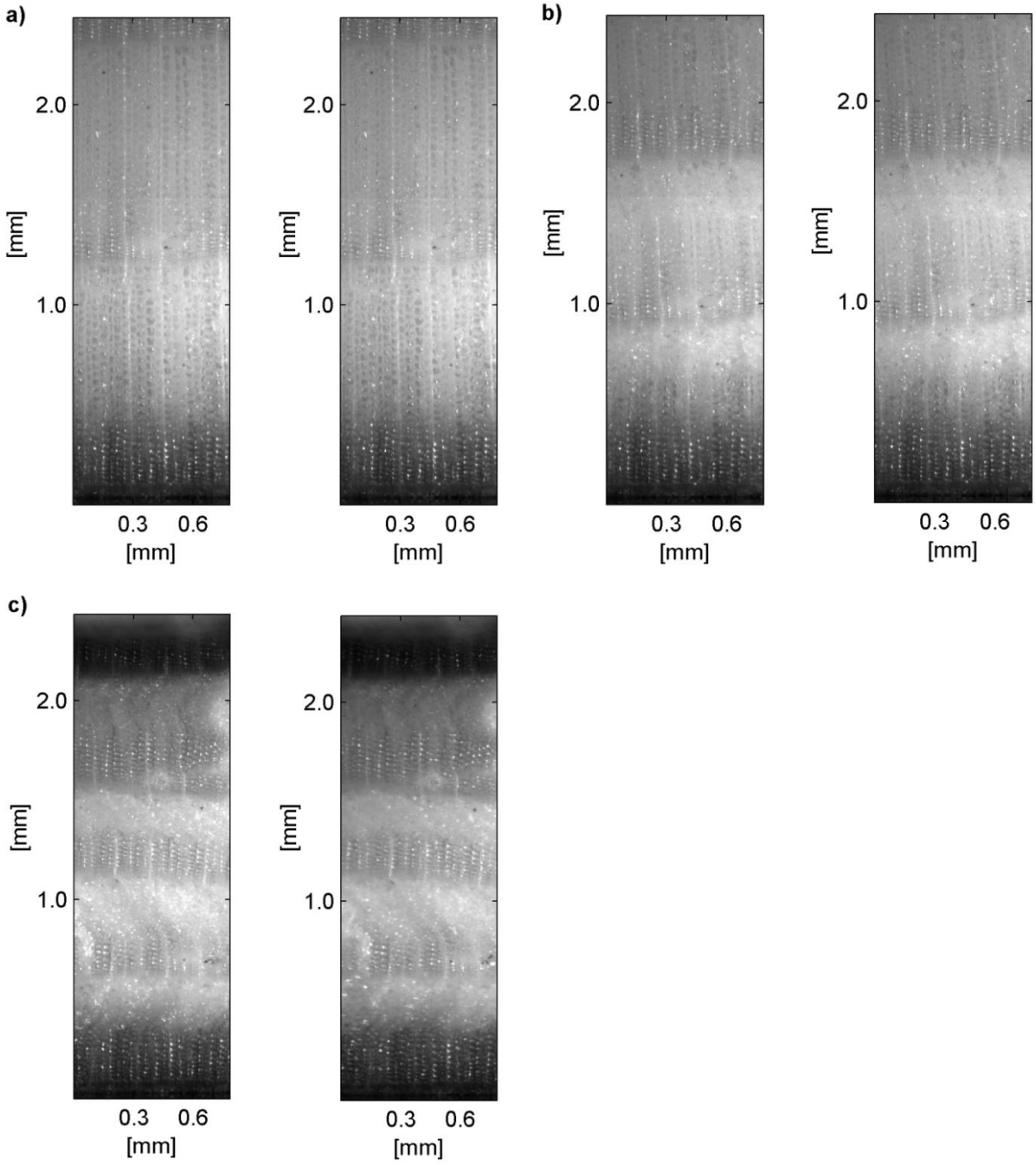

Fig. 13 Images from the cyclic compressions captured at positions a) I during the second and third compression cycles, b) II during the sixth and seventh compression cycles and c) III during the ninth and tenth compression cycles

In the stress strain curve of the advancing cyclic testing shown in Fig. 12a, we can see that the compressions move the yield limit (ε_y^{EW}) to the right and reduce the elastic modulus (E_e^{EW}). After the maximum strain of the previous compression, the compression progresses as in native wood. Furthermore, in Fig. 13 we can see that the cells have collapsed identically the second time the compression reaches the same strain level. Based on the result that the upper part of the cyclic curve corresponds to that of native wood subjected to one single compression it is reasonable to assume that the same stress strain pairs and identical cell collapse would have been achieved in the captured points if

the point would have been reached in one single compression. This implies that the energy used in previous cycles has not had any effect on the achieved fatigued state i.e. the previous cycles has only wasted energy due to internal material friction.

When the image based strain analysis for the cyclic test was finalized it could be concluded that the overall behavior of earlywood was the same as for average wood (registered by the testing equipment). However, Fig. 12b shows more clearly that the relaxation of the sample was incomplete (the compression cycles does not return to zero). The piston was raised to the initial position after every cycle but the sample did not relax back completely. The image series in this case was very long and the uncertainty was probably increased due to the accumulation of measurement noise.

The results from the cyclic earlywood compressions show how the wood was softened by each compression. The calculated value for the elastic modulus E_e^{EW} is plotted as a function of the compression number in Fig. 14a and as a function of the maximum strain of the previous compression in Fig. 14b for all of the compression cycles in Fig. 12b.

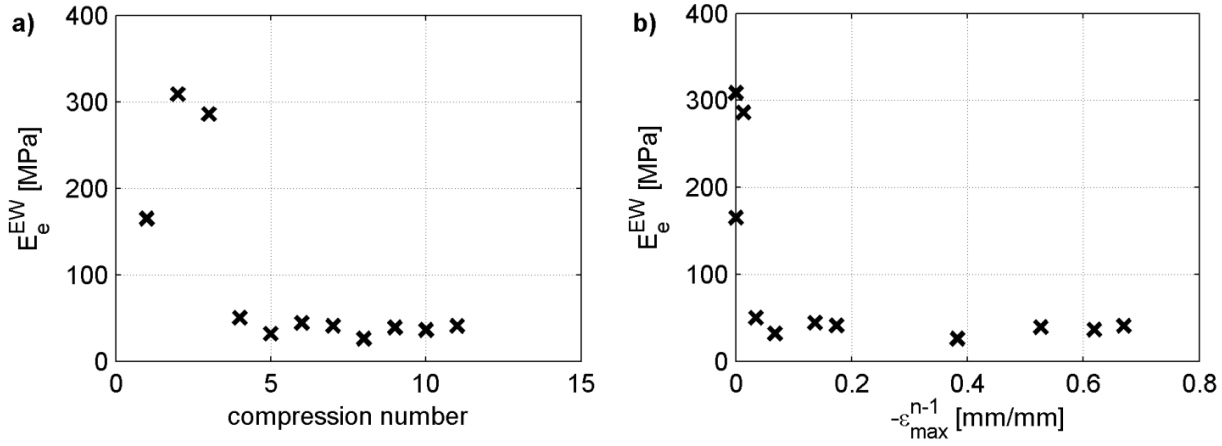

Fig. 14 The elastic modulus E_e^{EW} as a function of a) compression number and b) maximum strain of the previous compression.

The analysis behind the points in Fig. 14 was based on the testing of one single sample and the uncertainty is therefore rather large. On the other hand the upper part of the cyclic curve in Fig. 12 corresponds to that of native wood subjected to one single compression which indicates that the sample has been rather representative. The image series was significantly longer than the tests with one single compression. The elastic modulus of the compressions 2 and 3 are larger than the initial elastic modulus, which is theoretically unlikely and was probably caused by an insufficient relaxation time offered by the test cycle. Fig. 14 shows that the elastic modulus was reduced immediately after a few advancing strain cycles. In this test an average earlywood strain level of approximately 0.05 was sufficient to drop the elastic modulus to bottom level. This information would be relevant if the strain would be equally distributed in the sample. According to Fig. 13 this is not the case and therefore the local strain level needed for local elastic modulus drop is much higher.

The effect of fatigue for the wood compression models was studied by analyzing samples pre-treated with high strain rate compressions in both quasi static and high strain rate compression tests at room temperature and high temperature. The compression model was also fitted for the pre-fatigued samples. In [12], the compression behavior of pre-fatigued wood has been modelled with an additional region before the yield limit where the pre-fatigued fibers collapse. Here, the model used for fatigued wood had the same structure as that of native wood, with an initial linear elastic region up to the yield limit and thereafter a plateau region. This was chosen in order to simplify material modelling and later the model utilization, especially the transition from native to fatigued wood in wood behavior simulations.

Earlywood model. Stress strain curves at both temperatures for pre-fatigued wood based on the quasi static model and experimental data are presented in Fig. 15. In Figs. 16 and 17, the stress strain curves at both temperatures for pre-fatigued wood based on the dynamic model is presented and model fitted based on the quasi static model are included for comparison. The dynamic model curve overlaps the quasi static model curve in Fig. 17, which therefore cannot be seen.

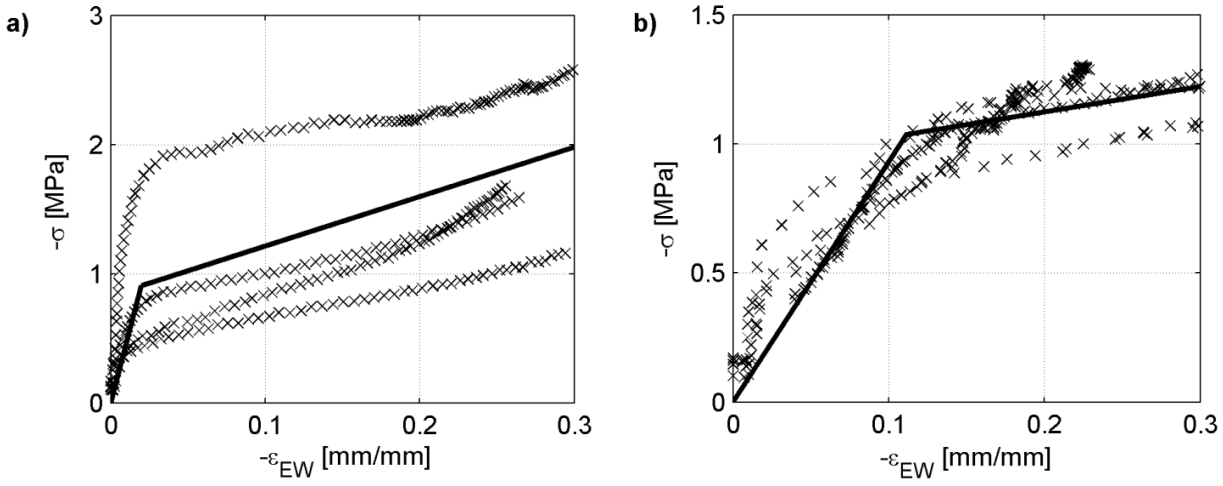

Fig. 15 Stress strain curves based on the quasi static earlywood model for pre-fatigued wood (solid line) and experimental data (x) from compression tests at a) room temperature and b) high temperature.

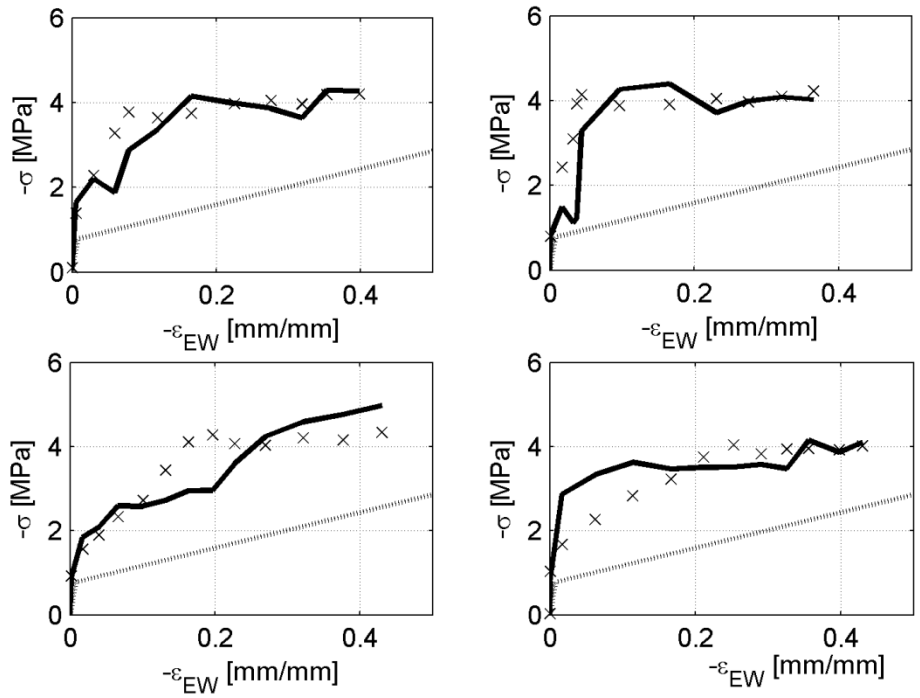

Fig. 16 Stress strain curves at room temperature for earlywood based on the dynamic model (solid line), the quasi static model (dotted line) and experimental data (x) from high strain rate testing of four pre-fatigued samples.

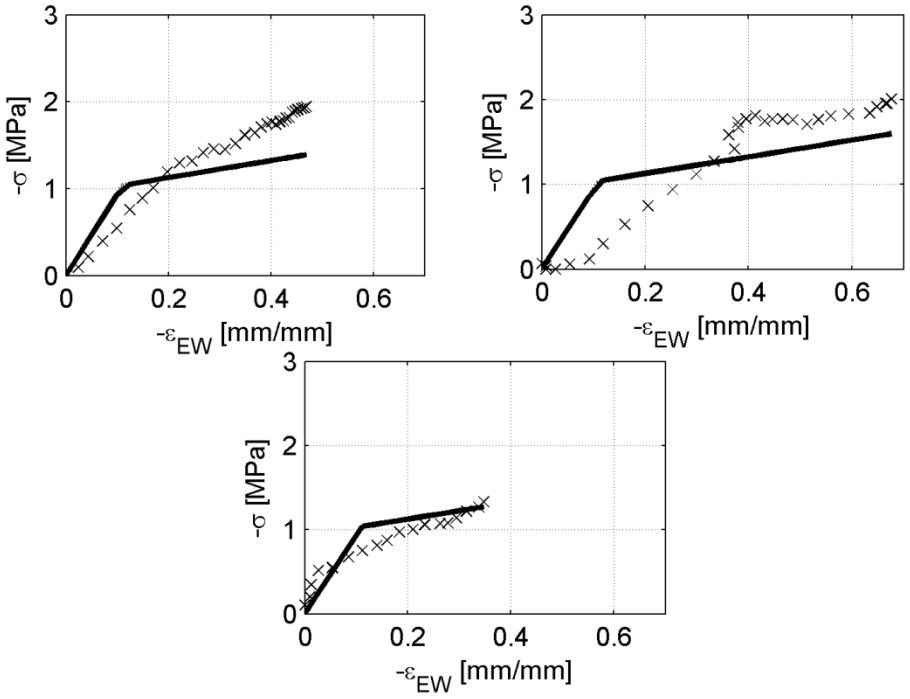

Fig. 17 Stress strain curves at high temperature for earlywood based on the dynamic model (solid line), the quasi static model (dotted line) and experimental data (x) from high strain rate testing of three pre-fatigued samples.

The pre-fatigue treatment has softened the earlywood which can be seen as lower dynamic modulus than in the case for native wood. The temperature rise is though dominant as its effect on the modulus is higher than the effect of pre-treatment. At low temperature there is a significant impact of the strain rate but at high temperatures the high strain rate model is practically equal to the quasi static model. The low amount of samples can have an influence on the result.

Latewood model. Quasi static models at both temperatures for fatigued latewood are presented together with experimental data in Fig. 18 and dynamic models at both temperatures for fatigued latewood are presented in Figs. 19 and 20. Quasi static models are also included in Figs. 19 and 20 to show the difference between the models.

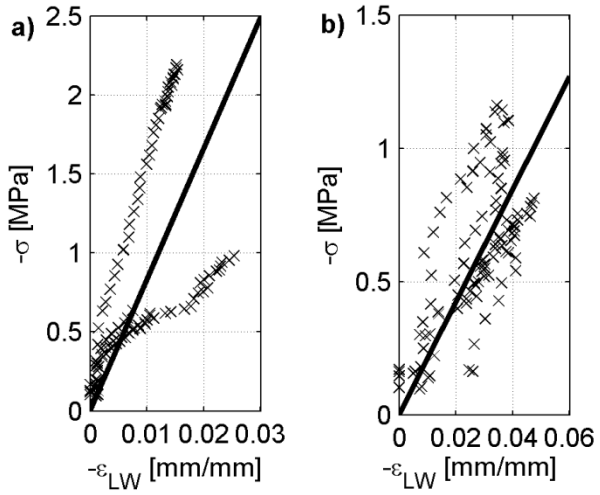

Fig. 18 Stress strain curves based on the quasi static latewood model for pre-fatigued wood (solid line) and experimental data (x) for compression at a) room temperature and b) high temperature.

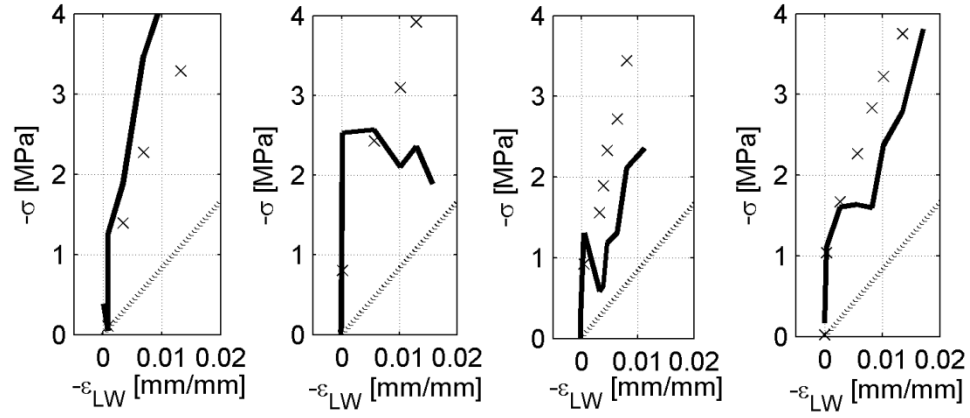

Fig. 19 Stress strain curves at room temperature for latewood based on the dynamic model (solid line), the quasi static model (dotted line) and experimental data (x) for high strain rate testing of four fatigued samples.

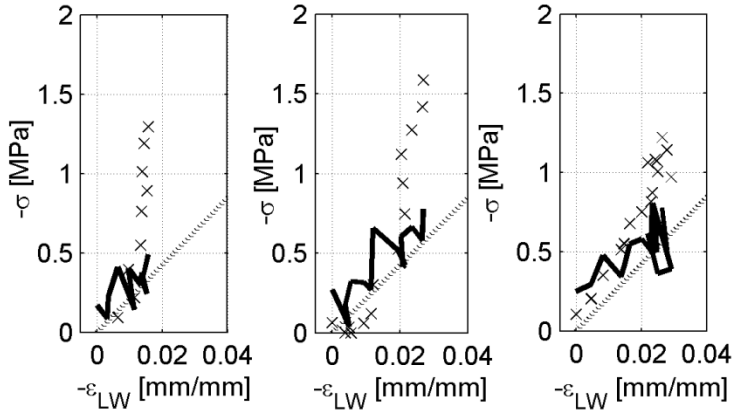

Fig. 20 Stress strain curves at high temperature for latewood based on the dynamic model (solid line), the quasi static model (dotted line) and experimental data (x) for high strain rate testing of three fatigued samples.

The pre-fatigue treatment has also softened the latewood which can be seen as significantly lower dynamic modulus than in the case for native wood. The temperature rise is also in this case dominant as its effect on the modulus is higher than the effect of pre-treatment. At low temperature there is a significant impact of the strain rate but at high temperatures the impact is smaller.

INITIAL SIMULATION OF MULTILAYERED COMPRESSION

Utilization of the modelled wood behavior is here demonstrated in an example, which is a simulation of strain compression of multiple year rings wood pieces at fiber saturated moisture content (~30 %) and at room temperature. The simulation model was implemented in a finite element method (FEM) software. Here the Solid Mechanics Module of Comsol Multiphysics was utilized where late wood was modelled as a linear elastic material and earlywood as an elastoplastic material. The simulation result is shown in Fig. 21 and compared to a similar real experiment in Fig. 22.

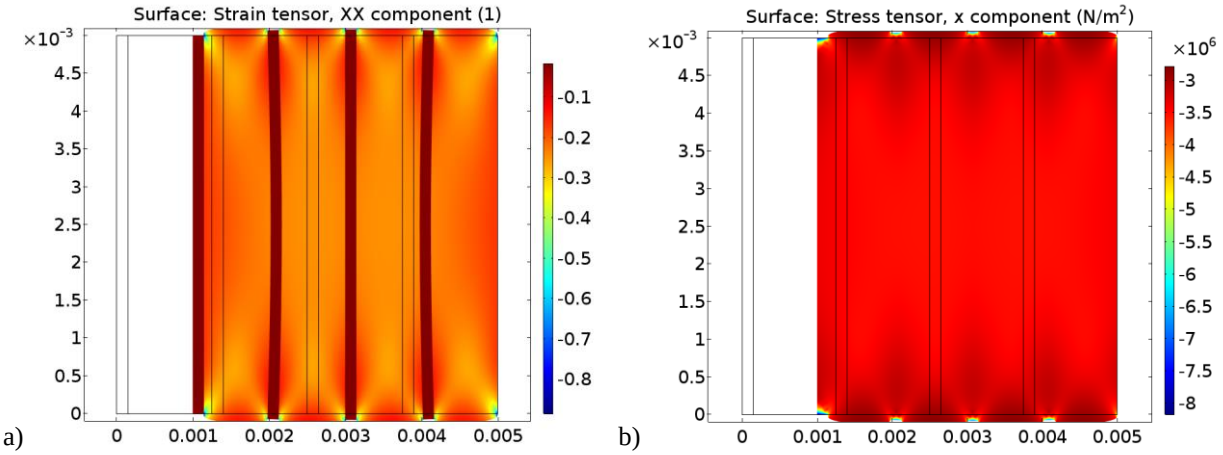

Fig. 21. Quasi static simulated radial compression based on the wood model in equations 1 and 2 at room temperature for an artificial sample (5 mm x 5 mm) containing four year rings. The sample is compressed 1 mm from left, giving an average strain of -0.2, a) the strain distribution between latewood and earlywood, and b) the mainly uniform stress of approximately -3.5 MPa.

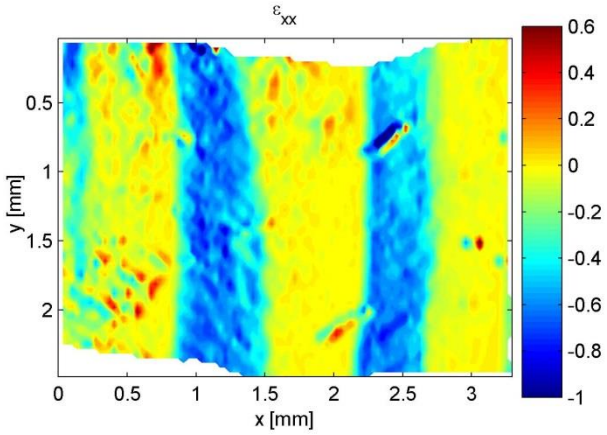

Figure 21. Quasi static measured radial compressive strain for a sample measured at room temperature at average strain of -0.21.

The average stress in the simulation was -3.5 MPa while the maximum stress in the end of measurement example was -3.4 MPa. As also the average strain is on the same level in both cases the modelling and simulation seems to be adequate. The figures though show that the strain distribution in the measured sample reaches higher strain values than corresponding values in the simulated distribution. The figures also show that the non-compressed areas are wider in the measured example than in the simulated example. The reason for the differences is that transition wood is not included in the modelling and that parts of the transition wood have not collapsed in the measurement example. The simulated example however represents a method which can be further developed for virtual energy efficiency optimization of mechanical pulping.

CONCLUSIONS

A dynamic wood compression model has been developed as parameters of the Voigt-Kelvin solid. The elastic effect is modelled by multiple regions using local strain in earlywood and latewood respectively. The viscous effect present at high strain rate is modelled by a strain rate dependent parameter also using the local strain rate in earlywood and latewood respectively. The effect of fatigue treatment and temperature increase can be roughly seen in the model tests

for native and fatigued wood measured at room temperature and high temperature. The presented model is the first wood compression behavior model individually for earlywood and latewood that is based on wood experiments where wood moisture, wood temperature and wood strain rate are at similar levels as in industrial defibration. A drawback in quasi static measurements is the lack of data at maximum pulping temperature e.g. 135 °C, due to the fact that the equipment could not be pressurized. The consequence is that the models presented here do not cover temperatures up to 135 °C even though high strain rate measurements up to 135 °C are presented in [12].

The advancing cyclic compression experiment showed clearly that identically repeating strain does not increase fatigue, either as new collapse patterns on fiber level or as lowered elastic modulus. The same experiment also indicates that enough large single compression strain pulses should be offered by defibration tools to reach high efficiency in internal fibrillation.

Energy efficient internal and external defibration is the final goal in mechanical pulping. Wood behavior modelling on the level of strain and stress does not directly reveal level of internal and external defibration. However strain and stress development can be used to estimate these levels. E.g. drop in elasticity modulus can be connected to internal fiber defibration and fiber surface stress caused by defibration tool could be connected to external fiber defibration.

A significant amount of work would be required to present the material parameters more accurately as functions of temperature and fatigue state. This entails high strain rate and quasi static material testing at additional temperatures and of additional pre-fatigue states. However, the presented dynamic compression model has already shown to be practical in initial multilayered compression simulations and will be very useful for simulations of wood behavior in the mechanical pulping process.

ACKNOWLEDGEMENTS

The Academy of Finland is acknowledged for the funding of the project Woodmat (decision number 140462), in which this research has been conducted. The Swedish Knowledge Foundation and the member companies of the E2MP-Research Profile at Mid Sweden University are also acknowledged for supporting this research. M. Ovaska, A. Miksic and M. Alava are supported by the Academy of Finland through its Centres of Excellence Programme (2012-2017 under project no. 251748). The authors are also grateful for the assistance with the high strain rate material testing by Max Lundström and Staffan Nyström in the Mid Sweden University Materal's Lab.

REFERENCES

1. Atack, D., Pye, I.T., (1964) The measurement of grinding zone temperature. Pulp and Paper Magazine of Canada 65(1964): T363-T376
2. Atack D., Clayton D.L., Quinn A.E. and Stationwala M.I., (1984) SPIE High Speed Photography (Strasburg), "High Speed Photography of Wood Pulping in a Disc Refiner", 491:348-353 (1984)
3. Alahautala T., Vattulainen J. and Hernberg R., (1997) XIV IMEKO World Congress, "Visualisation of Pulp Refining in a Rotating Disk Refiner", XA:60-64, 1997
4. Karlström, A., Eriksson, K. och Hill, J. (2015) Refiner optimization and control Part IV: Long term follow up of control performance in TMP processes. Nordic Pulp & Paper Research Journal (0283-2631). Vol. 30 (2015), 3, p. 426-435
5. Fredrikson, A. & Salminen, L.I. (2012) Analysis method of high-consistency chip refiner forces. Nordic Pulp and Paper Research Journal 2012, Vol. 27, No. 4 pp. 695-701
6. Becker, H., Noack, D., (1968) Studies on dynamic torsional viscoelasticity of wood. Wood Science and Technology, 1968, Vol. 2, 213-230
7. Höglund, H., Tistad, G., (1973). Energy uptake by wood in the mechanical pulping process. International mechanical pulping Conference, Stockholm 1973, Proceedings pp. 1-25
8. Höglund, H., Sohlin, U., Tistad, G., (1976). Physical properties of wood in relation to chip refining. Tappi, 1976, Vol. 59, No. 6, pp 144-147
9. Widehammar S (2004) Stress-strain relationships for spruce wood: Influence of strain rate, moisture content and loading direction. Exp Mech 44:44-48
10. Holmgren S, Svensson BA, Gradin PA, Lundberg B (2008) An encapsulated split Hopkinson pressure bar for testing of wood at elevated strain rate, temperature, and pressure. Exp Tech 32:44-50

11. Moilanen CS, Saarenrinne P, Engberg BA, Björkqvist T (2015) Image based stress and strain measurement of wood in the split-Hopkinson pressure bar. Meas Sci Tech 26:085206. doi: 10.1088/0957-0233/26/8/085206
12. Moilanen CS, Björkqvist T, Engberg BA, Salminen LI, Saarenrinne P (2016a) High strain rate radial compression of Norway spruce earlywood and latewood. Cellulose 23:873-889. doi: 10.1007/s10570-015-0826-5
13. Moilanen CS, Björkqvist T, Ovaska M, Koivisto J, Miksic A., Engberg BA, Salminen LI, Saarenrinne P, Alava M. (2016b) Influence of strain rate, temperature and fatigue on the radial compression behaviour of Norway spruce, submitted to Holzforschung
14. Persson K (2000) Micromechanical modelling of wood and fibre properties. Doctoral thesis, Lund University
15. Björkqvist T (2002) A design method for an efficient fatigue process in wood grinding - an analytical approach, Doctor of Technology, Tampere University of Technology
16. Hanhijärvi A., Mackenzie-Helnwein P. (2003) Computational analysis of quality reduction during drying of lumber due to irrecoverable deformation. I: Orthotropic viscoelastic-mechanosorptive-plastic material model for the transverse plane of wood. J Eng Mech 129:996-1005. doi: 10.1061/(ASCE)0733-9399(2003)129:9(996)
17. Somboon P, Nieminen K, Paulapuro H (2008) Finite element analysis of the fatigue behavior of wood fiber cell walls. BioResources 3(4), 983-994
18. Isaksson, P. , Gradin, P. A. & Hellström, L. M. (2013). A numerical and experimental study regarding the influence of some process parameters on the damage state in wood chips. Holzforschung, vol. 67: 6, ss. 691-696
19. Salmén L, Tigerstrom A, Fellers C (1985) Fatigue of Wood - Characterization of Mechanical Defibration. J Pulp Pap Sci 11:68-73
20. Salmén L (1987) The Effect of the Frequency of a Mechanical Deformation on the Fatigue of Wood. J Pulp Pap Sci 13:23-28
21. Salmén L, Dumail JF, Uhmeier A (1997) Compression behaviour of wood in relation to mechanical pulping. International Mechanical Pulping Conference:207-211
22. Björkqvist T, Lautala P, Saharinen E, Paulapuro H, Koskenhely K, Lönnberg B (1999) Behaviour of spruce sapwood in mechanical loading. J Pulp Pap Sci 25:118-123
23. Salmi A, Salminen LI, Engberg BA, Björkqvist T, Hæggström E (2012a) Repetitive impact loading causes local plastic deformation in wood. J Appl Phys 111. doi: 10.1063/1.3676206
24. Salmi A, Salminen LI, Lucander M, Hæggström E (2012b) Significance of fatigue for mechanical defibration. Cellulose 19:575-579. doi: 10.1007/s10570-011-9640-x
25. Lucander M, Asikainen S, Pöhler T, Saharinen E, Björkqvist T (2009) Fatigue treatment of wood by high-frequency cyclic loading. J Pulp Pap Sci 35:81-85
26. Salmi A, Salminen L, Hæggström E (2009) Quantifying fatigue generated in high strain rate cyclic loading of Norway spruce. J Appl Phys 106. doi: 10.1063/1.3257176
27. Gray III GT (2000) Classic Split-Hopkinson Pressure Bar Testing. In: Vol 8 Mechanical Testing and Evaluation, ASM Handbook. ASM International, pp 462-476
28. Gray III GT, Blumenthal WR (2000) Split-Hopkinson Pressure Bar Testing of Soft Materials. In: Mechanical Testing and Evaluation, Vol 8, ASM Handbook. ASM International, pp 488-496
29. Widehammar S (2002) A Method for Dispersive Split Hopkinson Pressure Bar Analysis Applied to High Strain Rate Testing of Spruce Wood, Department of Materials Science, Uppsala University
30. Kolsky H (1963) Stress Waves in Solids. Dover Publications Inc., New York